Automatic selection of color reference image for panoramic stitching

Muhammad Twaha Ibrahim, Rehan Hafiz, Muhammad Murtaza Khan & Yongju Cho

Multimedia Systems

ISSN 0942-4962

Multimedia Systems
DOI 10.1007/s00530-015-0467-4

Springer

Multimedia Systems
DOI 10.1007/s00530-015-0467-4

REGULAR PAPER

Automatic selection of color reference image for panoramic stitching

Muhammad Twaha Ibrahim[1] · Rehan Hafiz[1] · Muhammad Murtaza Khan[1,3] · Yongju Cho[2]

Received: 23 July 2014 / Accepted: 15 April 2015

Abstract Color correction is an important step in the generation of high-resolution stitched panoramas. Typically, color correction schemes try to match the color of each image in the panorama to an arbitrarily selected reference image. We provide a scheme that uses quantitative metrics such as image contrast, gradient-based structure similarity index measure (G-SSIM) and color clipping information to automatically select the best reference that results in visually pleasing output panoramas. Quantitative and qualitative evaluation of the scheme show encouraging results for panoramic images as well as for stitched videos. The scheme acts as a pre-processing step to color correction and its applicability to both parametric and non-parametric global color correction schemes has also been demonstrated.

Communicated by L. Zhang.

Electronic supplementary material The online version of this article (doi:10.1007/s00530-015-0467-4) contains supplementary material, which is available to authorized users.

✉ Rehan Hafiz
rehan.hafiz@seecs.edu.pk

Yongju Cho
yongjucho@etri.re.kr

[1] Vision Image and Signal Processing (VISpro) Lab, School of Electrical Engineering and Computer Science (SEECS), National University of Sciences and Technology (NUST), H-12, Islamabad 44000, Pakistan

[2] Broadcasting and Telecommunications Media Research Laboratory, Electronics and Telecommunications Research Institute, ETRI, Daejeon, Republic of Korea

[3] Faculty of Computer Science and Information Technology, University of Jeddah, Jeddah, Kingdom of Saudi Arabia

Keywords Image stitching · Color correction · Reference image selection · Panorama generation · Image registration

1 Introduction

Panoramic stitching is the process of seamlessly aligning and combining multiple images with overlapping fields of view to form a high-resolution output image [1]. Panoramic videos are generated using fish eye lens or by stitching together synchronized video frames acquired from multiple cameras arranged on a rig [2, 3]. Given the recent increase in the demand for viewing ultra-high definition content, the use of panoramas and high-resolution display systems that was once limited to geological surveys and surveillance applications [4] has now been extended for sports and entertainment industry [2, 5, 6]. For generation of a single panoramic image, the stitching process involves three main steps: geometric registration, photometric color correction and blending [1]. For panoramic videos, the relative camera arrangement is typically fixed and thus the geometric registration and color correction parameters are computed only once for initial frames. The computed corrections are then applied to subsequent frames as a batch process [3, 7].

Most color correction techniques [1, 8] arbitrarily select a reference image or require the user to choose one from among the images to be stitched [9]. The colors of the remaining images (often termed "target images") are modified to match the color palette of the selected reference image (I_{ref}). However, if the arbitrarily selected reference has poor color palette in terms of low brightness and contrast, the output panorama will also have poor colors making it visually unappealing. Figure 1 highlights the significance of selecting an appropriate image as I_{ref}. All the panoramas of Fig. 1 were created by stitching five images

Published online: 09 May 2015

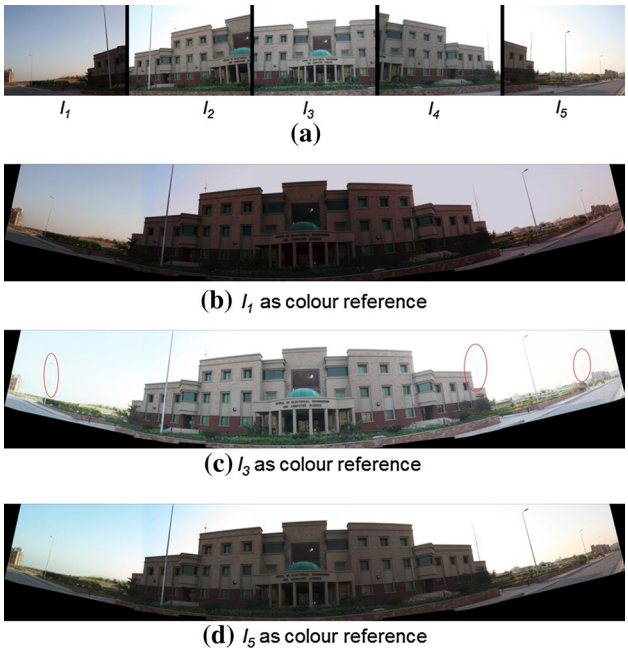

Fig. 1 **a** Source images forming the University Panoramas (**b**–**d**). The image selected as I_{ref} for performing color correction was different for each panorama in **b**–**d**

shown in Fig. 1a and while using the same color correction scheme, however the reference image I_{ref} was different for each panorama. Visually, panorama (b) is dull while panoramas (c) and (d) are more pleasing to look at. Thus arbitrary selection of I_{ref} can introduce undesirable effects independent of the selected color correction scheme. These artifacts may not go unnoticed for panorama use-case where ultimate aim is to provide rich in detail and high quality views using high-resolution monitors or large immersive multi-projector projection walls [10]. For example the panorama generation and rendering system by Fehn et al. [2] generated a live 5016 × 1400 panoramic video and projected it over a large cinema screen. The content was a live football match with a static soccer field as background. Recently introduced gigapixel panoramic videos [11, 12] provide another scenario where high-resolution stitched videos are being generated for static as well as moving scenes. The high resolution allows users to simultaneously view and zoom in the videos [13, 14]. Such large high-resolution display systems demand flawlessly stitched content since even a slight artifact in the structure or color of the panorama can degrade its visual plausibility.

To the best of our knowledge, this paper provides the first study which explicitly provides means for automatic selection and validation of the color reference image (I_{ref}) with the aim of generating a panorama with least structural and color artifacts. This work proposes the use of metrics such as image contrast, gradient-based structural similarity index measure (G-SSIM) [15] and a color clipping measure to automatically select the best reference. Section 2 highlights the need for an automatic reference selection scheme by providing a review of existing color correction schemes. Section 3 describes the proposed I_{ref} selection methodology. Section 4 provides detailed discussion on the results obtained after application of the scheme for panoramic images followed by a subjective evaluation that further demonstrates its usability for panoramic videos. Results for one non-parametric and two parametric color correction schemes are also provided followed by the conclusion in Sect. 5.

2 Literature survey

Color correction approaches can be divided into two broad categories: parametric and non-parametric [10]. Parametric approaches assume a relation between the colors of the target image and those of I_{ref}. On the contrary most non-parametric approaches use some form of a lookup table to record the mapping for the full range of color intensity levels [16, 17]. As stated in [9], whereas non-parametric approaches provide better color matching results in the overlapping region, parametric approaches are more effective in extending the color similarity to non-overlapping regions of the source images.

Color correction approaches are further classified as global schemes that assume a single relation between the reference and the target image, and local correction schemes. Local correction schemes typically make use of local content to transfer the colors from the selected reference image to a target image [18, 19]. Such techniques can improve the quality of color correction; however, they result in increased computational time for large datasets due to local processes such as segmentation. Xiong et al. [20] employed diagonal model [21] for color and luminance compensation in the framework of global color correction. In another work [22], they perform gamma correction for luminance component and linear correction for chrominance component by minimizing error functions based on pixel values in the overlapping regions. In a later work [23], the authors use dynamic programming to compute seams and blend images into the panorama using modified instant cloning. They compute the differences of the pixel values between the current panorama and the source image on the seam and distribute this color difference to the rest of the image by adding the color difference. In [8], the authors suggest a need for user input to select the best reference. However, they use a heuristic to select an image with the most similar means in R, G and B channels as the color reference. In Brown and Lowe [1] use gain compensation for reducing color differences between target and reference image forming the panorama. The gains are computed using an error function, which is the sum of gain normalized

intensity errors for all overlapping pixels. Doutre and Nasiopoulos [24] use a second-order polynomial to correct each pixel in the target image using the exposure and white balance of I_{ref}. The polynomial weights are computed by comparing the overlapping regions of images using standard linear least-squares regression. In [17] authors compute a brightness transfer function (BTF) by obtaining a joint histogram of the images. This joint histogram is determined by comparing the overlapping regions of adjacent images in a panorama. The BTF is computed for each of the RGB channels separately before being applied to the target images.

In almost all the techniques mentioned above, the color reference image for photometric correction of images, constituting the panorama, is either selected arbitrarily or chosen by the user. Arbitrary selection of I_{ref} may not always result in a visually pleasing output panorama. For example, in Fig. 1a, if image I_1 is chosen as color reference, then the output panorama of Fig. 1b is obtained, which is significantly dull. In case of user selection, the output will depend entirely upon the subjective evaluation of the user and thus, different users may end up choosing different references. Furthermore, when the colors of the images are matched to I_{ref}, it may result in undesirable effects such as loss of structure and clipping of colors due to the application of the color transfer function. Therefore, an objective evaluation metric is highly desirable for choosing a color reference. Xiong and Pulli [8] recommend using an image with the most similar means in R, G and B channels as I_{ref}. However, neither any analytical or experimental analysis provided to support this selection procedure nor any validation criteria are provided. Thus, to the best of our knowledge, this is the first formal effort to define an automatic, quantitative and analysis-based selection and verification criteria for selecting the best I_{ref} for panoramic color correction.

This work builds upon the authors' recent contribution [25] which provided a scheme to select the most appropriate I_{ref} for global parametric color correction schemes. In [25], the color correction coefficients for a global parametric color correction scheme are first computed using an arbitrarily selected I_{ref}. Next, the image with the minimum value of Ω, which is the sum of normalized transformed grayscale values over all the RGB channels are selected as the reference image (I_{ref}). For an image I_{i} among n images to be stitched:

$$\Omega(i) = \frac{1}{3} \sum_{k \in \text{R,G,B}} \frac{1}{255} \sum_{j=1}^{255} \frac{T(M_i, j)_{(k)}}{j} \tag{1}$$

$$\text{ref} = \arg\min(\{x : x = \Omega(i), 1 \leq i \leq n\}) \tag{2}$$

Here j, M_{i}, and T represent the grayscale values that can be represented in the image (0–255 for an 8-bit image), the color correction model parameters (e.g., the Diagonal plus Affine model [21]) and the color transfer function (which transforms an input grayscale value to an output grayscale value based on the color correction model), respectively. The color correction coefficients are then modified so that the colors of all target images match those of the I_{ref}. For example, assume that in a set of five images, the color correction coefficients are first computed and image I_3 is selected as reference since it has the least value Ω. The color coefficients are then modified to match the colors of all images to I_3. In case a subjective evaluation reveals significant amount of color clipping, the next image with least value of Ω is chosen as the reference.

The current work has notable differences as compared to the earlier work [25]. First, though the reference selection procedure was automatic, the evaluation for the selected reference was purely a subjective assessment. Second, the earlier technique was limited in application to global parametric color correction schemes only, since it was a function of the gains of the parametric color correction scheme. Third, unlike the current scheme, the earlier approach required the application of color correction scheme prior to determining the ranking metric (Ω). In this work, we not only provide a new improved metric for automatic selection of best reference image but also provide quantitative measures to automatically validate the selection after generation of panoramic image, thus requiring no manual input during the complete panorama generation phase.

3 Proposed methodology

Loss of image information is detrimental to the visual perception of an image [29]. Human visual system is particularly sensitive to the structural information contained in an image [26]. Furthermore, an image with higher contrast is typically perceived as having a higher visual quality [30]. Thus, we propose the I_{ref} to be the one whose selection results in the generation of a panorama having the following desirable characteristics:

1. *High contrast* A panorama with a higher contrast is more pleasing to look at since it assures higher level of details in the image. In this paper the standard deviation has been used as a metric for measuring image contrast as proposed in [16, 26].
2. *Preservation of edges* When images are corrected for color it is possible that edges become weak. This may happen due to two reasons: (i) the color transfer function maps different gray levels in the original image to similar gray levels in the output image (ii) the color transfer function results in clipping of color values. Both factors result in less discernable difference between similar intensity levels thus resulting in loss of edges. In this work we make use of gradient-

based SSIM (G-SSIM) [15] as a metric to highlight the preservation of edges by comparing the high frequency information in both original and color corrected images. The value of G-SSIM ranges from 0 to 1, where 1 represents an exact match.

3. *No significant clipping* Clipping of intensity levels can result in loss of details and color gradients. Clipping occurs when the color transfer function maps color value of any of the RGB channel to the maximum possible level (256 for an 8-bit image). In this paper clipping is measured by computing the percentage increase in the number of pixels with maximum gray level for all RGB channels (RGB) before and after color correction ($\Delta C_{\%age}$). A positive value of this measure indicates an increase in color clipping due to application of color correction with the selected $I_{\text{ref.}}$

These characteristics are applicable to both individual images and individual frames of a video panorama since they ensure that each frame of the video is visually pleasing to a certain level. Next, we explain the proposed methodology for automatically selecting the color reference.

3.1 Procedure for automatic color reference selection

The proposed methodology for automatically selecting the color reference comprises of three main steps. First, a metric, called D, is defined that ranks the suitability of each input image for being the reference in a descending ordered list. The metric D is based upon the standard deviations of the overlapping regions of adjacent images. Next, a global color correction scheme is applied on each image that matches its color to that of the reference image with highest value of D. The next step is to automatically validate this selection. For this, the color corrected images are compared to their corresponding uncorrected versions for any structural or color loss that may have been introduced as a result of the color transformation. In case the validation measures indicate structural or color loss, the current selection is invalidated and the procedure is repeated for the image with next highest value of D. The process is repeated until the validation criteria are met. The entire approach is summarized by the flowchart in Fig. 2 and described below.

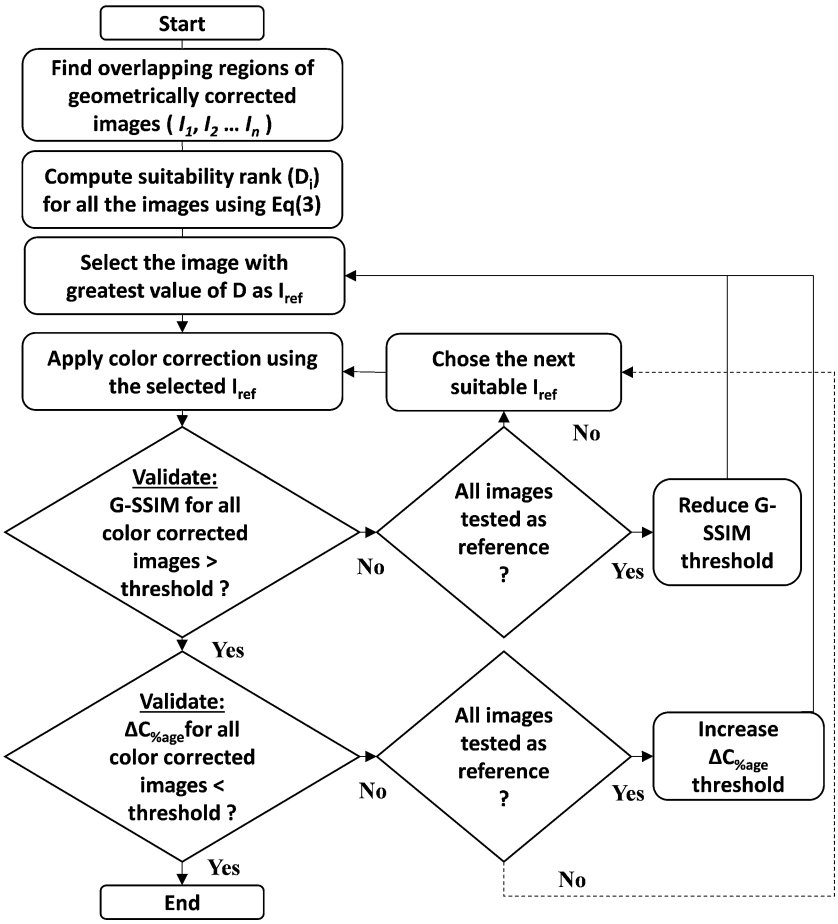

Fig. 2 Algorithmic flow of the proposed scheme

3.1.1 Determining the suitability rank D_i

Let I_1, I_2,…,I_n represent the images acquired from n different views where I_1 is the left-most image in the panorama. For panoramic videos I_1, I_2,…,I_n can be thought of as the first frame acquired by each camera. Most panorama color correction techniques compute the color transfer function using only the overlapping regions [1, 17, 21] since content is nearly identical for a geometrically corrected image pair. Thus, only the overlapping regions of the images are considered when computing the metric D_i for each image I_i. Let ($I_{i-1,0}$, $I_{i,0}$) denote the geometrically corrected overlapping regions of adjacent images I_{i-1} and I_i, respectively. The standard deviations of $I_{i-1,0}$ and $I_{i,0}$ are computed for the R, G and B channels separately. To rank all images in the context of their suitability as color reference image (I_{ref}), their standard deviations are compared. Since, D is a relative metric it is measured relative to I_1. Thus, the difference between the standard deviation of each image (I_i) from I_1 is computed by accumulating the pairwise percentage differences of all the images I_1, I_2,…,I_n. For an image pair ($I_{i-1,0}$, $I_{i,0}$) and their pairwise standard deviations $\sigma_{i-1,i}$, the percentage difference of the standard deviations of image I_i with respect to I_{i-1} is calculated for all image pairs:

$$D_i = \left\{ D_{i-1} + \text{sum}\left(\left(\frac{\sigma_i^j - \sigma_{i-1}^j}{\sigma_{i-1}^j} \right) \times 100 \right) \right\} \quad 2 \le i \le n, j \in R, G, B \tag{3}$$

where σ_i^j. and σ_{i-1}^j refer to the standard deviations of the jth channel of image $I_{i,0}$ and $I_{i-1,0}$, respectively. D_1 is assumed to be 0. This metric serves as an initial ranking of the images in order of their suitability as color references and the image with the highest value of D is chosen as reference. It is represented by I_{ref} and its index is given by:

$$\text{ref} = \arg\min(\{x : x = D_i, 1 \le i \le n\}) \tag{4}$$

3.1.2 Applying a color correction scheme

Next, the images are corrected for color by applying any parametric or non-parametric global color correction scheme with the automatically selected image I_{ref} as color reference. In this work we have provided the majority of results for Diagonal plus Affine model [21], a parametric color correction scheme, since it is recommended by [9]. Brightness transfer function [17], a non-parametric technique and gain compensation [1], a parametric technique are further examples of color correction schemes that may be employed.

3.1.3 Validating edge preservation and clipping avoidance

As shown in Fig. 2, the next step is to validate whether the selected I_{ref} results in a visually plausible panorama. We make use of G-SSIM and percentage clipping ($\Delta C_{\%\text{age}}$) for this validation.

To determine edge preservation, we compute gradient-based SSIM [15] between color corrected images and their original, uncorrected images. The SSIM proposed by Wang et al. [26] consists of three components: Luminance comparison $l(I^{\text{o}}, I^{\text{c}})$, contrast comparison $c(I^{\text{o}}, I^{\text{c}})$ and structure comparison $s(I^{\text{o}}, I^{\text{c}})$, where I^o represents the original, unmodified image and I^{c} represents the color corrected image. The SSIM is defined as:

$$\text{SSIM}(I^{\text{o}}, I^{\text{c}}) = \left[l(I^{\text{o}}, I^{\text{c}}) \right]^{\alpha} \times \left[c(I^{\text{o}}, I^{\text{c}}) \right]^{\beta} \times \left[s(I^{\text{o}}, I^{\text{c}}) \right]^{\gamma} \tag{5}$$

where $\alpha > 0$, $\beta > 0$ and $\gamma > 0$ are weights for each of the three components. The G-SSIM differs from SSIM in that the contrast and structure comparisons are applied on the image gradient maps rather than the original images. This is done by applying the sobel operator on the input images before computing these comparisons. The overall image quality can be evaluated by taking the mean of the G-SSIM values for each color channel. The higher the value of G-SSIM the more similar the images, with 1.0 representing an exact match.

To determine color clipping, we compute the percentage clipping ($\Delta C_{\%\text{age}}$) before and after the application of color correction for each image using Eq. (6):

$$\Delta C_{\%\text{age}_i} = \frac{1}{N \times M \times 3} \times \left\{ \sum_{k \in \text{R,G,B}} p(I_{i,k}^{\text{c}}, 255) - p(I_{i,k}^{\text{o}}, 255) \right\} \times 100 \quad 1 \le i \le n \tag{6}$$

where $p(I_{i,k}, j)$ returns the number of pixels of gray value j in the kth channel of image I_i, and N and M are the number of image rows and columns, respectively. I^{c} represents the color corrected image and I^{o} represents the original image.

As illustrated in Fig. 2, for a selected I_{ref}, all the color corrected images of the panorama image set are evaluated for edge loss. If the G-SSIM value for any color corrected image in this image sequence is less than a threshold (discussed in Sect. 4), the currently selected I_{ref} is discarded and the image with the next highest value of D is selected as I_{ref}. The color correction is applied again and the validation procedure is repeated. If there is no such I_{ref} that passes the validation criterion, the G-SSIM threshold is decreased by a step size (5 % in our experiments) and the process is repeated once again starting from the most suitable reference. In a similar manner, the criteria for percentage clipping ($\Delta C_{\%\text{age}}$) are evaluated. If the percentage change is greater than a certain threshold (discussed in Sect. 4) for any image in the image sequence, the currently selected color reference is discarded and the next most suitable reference based on D is selected. If there is no such reference, then the $\Delta C_{\%\text{age}}$ threshold is increased by a step size (5 %

in our experiments) and the process is repeated again starting from the most suitable reference. The procedure finishes once an I_{ref} meeting the validation criteria is found.

4 Results and discussion

In this section we provide an analysis of application of the proposed scheme on the image set of Fig. 1 followed by comparison of our proposed scheme to that of [8] and [25] for a number of cases by utilizing the parametric Diagonal plus affine color correction scheme [21]. The applicability of the proposed scheme for images and videos is also demonstrated via subjective evaluation. Finally, results of the scheme when used with a non-parametric color correction approach are also provided at the end.

We evaluated the proposed scheme for the University panorama image set of Fig. 1. Each row of Table 1 provides the value of a number of measures when a particular image is selected as reference I_{ref} and the colors of all other images (I_1–I_5) are matched to it. The first column shows the values of D_i, the proposed metric to determine the most suitable color reference. The image with the highest value of D_i is the suggested reference. For the University panorama, D suggests I_5 as the most suitable panorama with the largest score of 59.67 followed by scores of I_4, I_2, I_1 and I_3, respectively. In Table 1, the row highlighted in blue corresponds to the case when the most suitable image is selected as reference while red corresponds to the case when the least suitable image is selected as reference. The G-SSIM ($I_i^o I_i^c$) and percentage clipping $\Delta C_{\%i}$ values are also presented for all images, which are computed by comparing the color corrected images (I_i^c) with their original images (I_i^o) for each reference case using the method provided in Sect. 3.1.3. As an example, the row in Table 1 highlighted in blue shows that when I_5 is selected as color reference, the value of G-SSIM and $\Delta C_{\%\text{age}}$ measure between original I_1 and color corrected I_1 is found out to be 0.99 and 1.32, respectively. For the same row since I_5 is the selected reference, no color transformation is applied on I_5 itself and hence there is neither any structural change nor any color clipping. This is represented by the maximum possible G-SSIM value of 1 and $\Delta C_{\%\text{age}}$ value of 0. The last column shows σ_{pano}, the average of standard deviations over all the RGB channels of the output panorama. A higher value of standard deviation indicates higher image contrast. Thus, when I_5 is selected as reference, the output panorama has a σ_{pano} value of 28.06. Note that the panorama in Fig. 1b, with I_1 as I_{ref} is significantly dull compared to Panoramas (c) and (d), whose references are I_3 and I_5 in Fig. 1a, respectively. While panorama (c) shows a brighter output, loss of details (lamp posts and transmission tower marked in red) can be observed. Table 1 reveals this fact as well. Notice that the G-SSIM value of color corrected image I_5 when image I_3 is set as reference is 0.87. This relatively lower value complies with the visual analysis as the transmission tower and lamp post are barely visible in panorama of Fig. 1c. The higher values of $\Delta C_{\%\text{age}}$ for color corrected image I_5 when image I_3 is used as reference indicates the presence of clipping in the resulting panorama, which can be noticed towards the right portion of panorama of Fig. 1c. Thus, as suggested by the value of D for I_5, the panorama of Fig. 1d provides the best output quality with maximum contrast, while preserving edges and having no significant clipping. The analysis further elaborates that G-SSIM, $\Delta C_{\%\text{age}}$ and σ_{pano} are insightful measures and hence are used later in this section when comparing results with the schemes of [8] and [25].

4.1 Results for panoramic images

A number of test cases for panoramic images were acquired using a circular rig of five SONY FS100 cameras. The proposed scheme was evaluated for a number of panoramas and its efficacy compared with [8, 25] for parametric color correction scheme of [21]. In [8], the authors select an image with the most similar RGB means as color reference. As a measure of similarity, standard deviation of RGB means has been used and the image with the least value of standard deviation of RGB means is selected as reference by [8]. The symbol η is used in this paper to represent this metric of [8]. For [25], the order of most suitable reference is determined by ascending order of the computed metric (Ω). Due to constraints of space, results generated from six panoramic sets (Figs. 3, 4, 5, 6, 7, 8) are provided in Tables 2, 3, 4, 5, 6 and 7. Since there is no

Table 1 D, G-SSIM and $\Delta C_{\%\text{age}}$ and σ_{pano} values for University Panorama of Fig. 1 for each possible selection of I_{ref}

I_{ref}	D	G-SSIM					$\Delta C_{\%\text{age}}$					σ_{pano}
		I_1	I_2	I_3	I_4	I_5	I_1	I_2	I_3	I_4	I_5	
I_1	0	1	0.73	0.62	0.85	0.99	0	−11	−17	−31	−22	22.89
I_2	4.41	0.88	1	0.98	0.98	0.91	3.1	0	0	0.34	5.92	23.84
I_3	−13.58	0.82	0.98	1	0.95	0.87	4.4	3.9	0	0.57	5.92	21.60
I_4	14.53	0.92	0.98	0.95	1	0.96	1.4	−11	−18	0	3.8	24.70
I_5	59.67	0.99	0.96	0.95	0.91	1	1.32	−11	−17	0	0	28.06

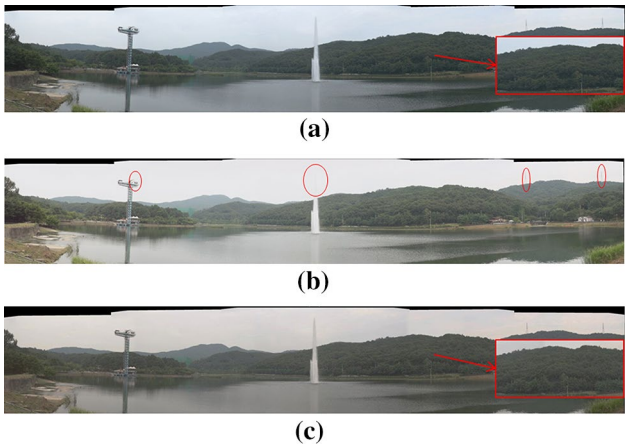

Fig. 3 Generated fountain panoramas when: **a** I_1 (ranked most suitable), **b** I_5 (ranked least suitable) and **c** I_3 is selected as I_{ref}, respectively

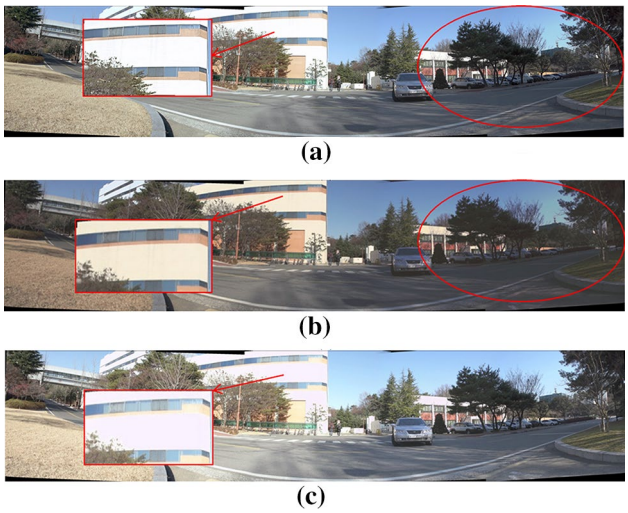

Fig. 4 Generated Office building panoramas when: **a** I_4 (ranked most suitable by proposed scheme), **b** I_1 (selected by [8]) and **c** I_5 is selected as I_{ref}, respectively

ground truth available for the selection of best reference, we compare the values of G-SSIM, $\Delta C_{\%\text{age}}$ and σ_{pano} for all possible references, i.e., for the case when I_1, I_2, I_3, I_4 or I_5 is selected as reference. Furthermore, for each image set, notable observations in the generated panoramas are discussed in relation to the computed values of SSIM, $\Delta C_{\%\text{age}}$ and σ_{pano}.

Similar to Tables 1 and 2 provides the values of η (the measure of [8]), Ω (the measure of [25]), D (proposed measure), Entropy E, G-SSIM, $\Delta C_{\%\text{age}}$ and σ_{pano} for each possible selection of color reference. For Fountain panorama of Fig. 3, η and Ω rank the suitability in the ascending order while D ranks the suitability in descending

Fig. 5 Generated Baseball stadium panoramas when: **a** I_5 (ranked most suitable by proposed scheme [8] and [25]) and **b** I_3 (least suitable) is selected as I_{ref}, respectively

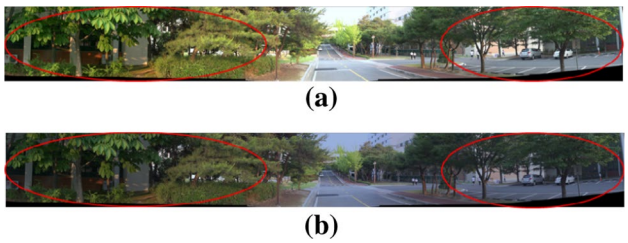

Fig. 6 Generated Street panoramas when: **a** I_5 (ranked most suitable by proposed scheme) and **b** I_2 (selected by [8]) is selected as I_{ref}

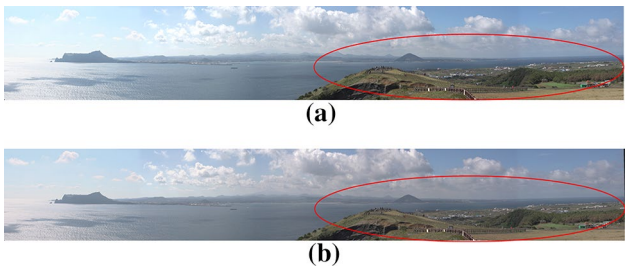

Fig. 7 Generated Island panoramas when: **a** I_4 (ranked most suitable by proposed scheme) and **b** I_5 (selected by [8]) is selected as I_{ref}

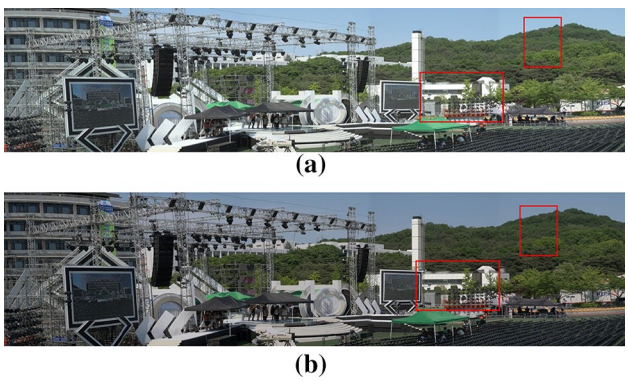

Fig. 8 Generated Island panoramas when: **a** I_5 (ranked most suitable by proposed scheme and [8]) and **b** I_4 (least suitable) is selected as I_{ref}

Table 2 Values of η (measure of [8]), Ω (measure of [25]), D (proposed measure), Entropy E, G-SSIM, $\Delta C_{\%age}$ and σ_{pano} for each possible selection of color reference (I_{ref}) for Fountain panorama of Fig. 3

I_{ref}	η [8]	Q [25]	D	E	G-SSIM					$\Delta C_{\%age}$					σ_{pano}
					I_1	I_2	I_3	I_4	I_5	I_1	I_2	I_3	I_4	I_5	
I_1	16.05	1	0	2.26	1	0.99	0.99	0.98	0.97	0	0	0	0	0	4.79
I_2	6.36	1.09	−15.07	3.64	0.99	1	0.99	0.98	0.97	0	0	0	0	0	4.54
I_3	16.43	1.06	−6.58	6.13	0.99	0.99	1	0.99	0.97	0	0	0	0	0	4.65
I_4	11.39	0.45	−33.12	4.58	0.99	0.95	0.96	1	0.99	0	0	0	0	0	4.25
I_5	9.24	0.25	−36.03	3.89	0.99	0.9	0.91	0.99	1	0	0	0	0	0	4.28

Table 3 Values of η ([8]), Ω ([25]), D, G-SSIM, $\Delta C_{\%age}$ and σ_{Pano} for each possible selection of I_{ref} for office building panorama of Fig. 3

I_{ref}	η [8]	Q [25]	D	G-SSIM					$\Delta C_{\%age}$					σ_{pano}
				I_1	I_2	I_3	I_4	I_5	I_1	I_2	I_3	I_4	I_5	
I_1	15.47	1	0	1	0.99	0.99	0.92	0.87	0	−0.05	−0.05	−0.11	−1.6	10.69
I_2	16.35	0.86	9.03	0.99	1	0.98	0.98	0.96	0.23	0	−3.7	−0.11	−1.5	10.97
I_3	23.21	1.11	5.32	0.99	0.99	1	0.95	0.87	0	−0.05	0	−0.11	−1.5	10.95
I_4	23.26	0.98	107.15	0.95	0.96	0.96	1	0.97	1.2	2.4	14.5	0	−1.5	12.07
I_5	25.88	0.78	140.76	0.89	0.91	0.87	0.97	1	0.48	1.7	19.4	6.5	0	11.46

Table 4 Values of η ([8]), Ω ([25]), D, G-SSIM, $\Delta C_{\%age}$ and σ_{pano} for each possible selection of I_{ref} for baseball stadium panorama of Fig. 5

I_{ref}	η [8]	Q [25]	D	G-SSIM					$\Delta C_{\%age}$					σ_{pano}
				I_1	I_2	I_3	I_4	I_5	I_1	I_2	I_3	I_4	I_5	
I_1	16.5	1	0	1	0.99	0.99	0.99	0.99	0	0.25	0.08	−0.02	−0.16	11.52
I_2	8.87	1.09	−10.81	0.98	1	0.99	0.99	0.98	0.06	0	0	−0.02	−0.16	11.42
I_3	10.3	1.02	−11.37	0.98	0.99	1	0.99	0.99	0.06	0	0	−0.02	−0.16	11.34
I_4	11.61	0.94	11.94	0.99	0.99	0.99	1	0.99	0.66	0.51	0.53	0	−0.16	12.02
I_5	8.21	0.86	21.23	0.99	0.98	0.99	0.99	1	3.06	6.66	3.31	0.11	0	12.14

Table 5 Values of η ([8]), Ω ([25]), D, G-SSIM, $\Delta C_{\%age}$ and σ_{pano} for each possible selection of I_{ref} for the street panorama of Fig. 6

I_{ref}	η [8]	Q [25]	D	G-SSIM					$\Delta C_{\%age}$					σ_{pano}
				I_1	I_2	I_3	I_4	I_5	I_1	I_2	I_3	I_4	I_5	
I_1	21.58	1	0	1	0.93	0.98	0.99	0.99	0	0.9	12.4	6.07	2.17	13.18
I_2	13.61	1.99	−80.66	0.92	1	0.97	0.97	0.92	−0.04	0	−0.13	−0.31	−0.26	12
I_3	34.29	1.59	−1.58	0.98	0.97	1	0.99	0.99	−0.04	0.45	0	−0.25	−0.25	14.3
I_4	27.24	1.71	7.92	0.99	0.96	0.99	1	0.99	−0.04	0.52	−0.1	0	−0.26	14.78
I_5	24.85	1.7	31.32	0.99	0.95	0.99	0.99	1	−0.04	0.61	4.79	1.36	0	15.64

Table 6 Values of η ([8]), Ω ([25]), D, G-SSIM, $\Delta C_{\%age}$ and σ_{pano} for each possible selection of I_{ref} for the Island panorama of Fig. 7

I_{ref}	η [8]	Q [25]	D	G-SSIM					$\Delta C_{\%age}$					σ_{pano}
				I_1	I_2	I_3	I_4	I_5	I_1	I_2	I_3	I_4	I_5	
I_1	18.01	1	0	1	0.99	0.99	0.99	0.99	0	0.66	0.19	−0.05	0.03	9.7
I_2	17.42	1.42	31.67	0.99	1	0.99	0.99	0.99	−7.8	0	0.16	−0.06	0.03	10.83
I_3	15.61	1.47	27.98	0.99	0.99	1	0.99	0.99	−7.8	−1.6	0	−0.05	0.01	10.71
I_4	8.59	1.41	39.14	0.99	0.99	0.99	1	0.99	2.5	4.1	0.46	0	0.01	11.26
I_5	7.7	1.49	20.05	0.99	0.99	0.99	0.99	1	−7.8	−1.6	−0.08	−0.05	0	10.39

order. Thus, in Table 2, the method proposed by [8] sets the most suitable order as I_2, I_5, I_4, I_1 and I_3. [25] sets the most suitable reference image order as I_5, I_4, I_1, I_3 and I_2, whereas the proposed metric D selects the order of the most suitable reference order as I_1, I_3, I_2, I_4 and I_5. The most and least suitable I_{ref} according to each of these

Table 7 Values of η ([8]), Ω ([25]), D, G-SSIM, $\Delta C_{\%age}$ and σ_{pano} for each possible selection of I_{ref} for the Concert panorama of Fig. 8

I_{ref}	η [8]	Q [25]	D	G-SSIM					$\Delta C_{\%age}$					σ_{pano}
				I_1	I_2	I_3	I_4	I_5	I_1	I_2	I_3	I_4	I_5	
I_1	10.5	1	0	1	0.99	0.99	0.98	0.99	0	3.5	0.01	4.3	0.01	9.11
I_2	18.41	0.89	−35.59	0.99	1	0.99	0.99	0.98	−0.01	0	0	3.1	−0.02	8.74
I_3	13.5	1.08	−6.03	0.99	0.99	1	0.99	0.98	−0.01	0.34	0	3.9	−0.02	9.52
I_4	10.97	1.58	−53.89	0.96	0.99	0.97	1	0.97	−0.01	0	0	0	−0.02	8.1
I_5	9.5	1.15	14.8	0.99	0.99	0.99	0.97	1	−0.01	0.46	0	4.22	0	9.62

schemes is highlighted in Table 2 in blue and red, respectively. It can be observed that I_{ref} selected by [25] and [8] result in panoramas with lower σ_{pano} while reference selection using D provides the panorama with maximum σ_{pano}.

Panoramas in Fig. 3 provide further support to our automatic selection of I_1 as reference. Panoramas in a, b and c correspond to the cases when I_1, I_5 and I_3 are selected as reference, respectively. According to the proposed measure, I_1 is the most suitable while I_5 is the least suitable color reference. It can be observed that the fountain tip is no longer clear in the panorama of Fig. 3b whereas it is visible in Fig. 3a. This observation can be related to the G-SSIM values in Table 2 when I_5 is selected as reference. When image I_3 (containing the fountain) is matched to I_5's colors, the G-SSIM value is 0.91, indicating a significant loss of image edges. When I_2 is matched to the color of I_1 it results in a G-SSIM measure of 0.99. On the contrary, when it is matched to that of I_5, it results in a G-SSIM measure of 0.90 representing loss of edges. This can be observed in Fig. 3b where the edges of the hut above the tower are almost merged with the sky while these edges are clearly visible in Fig. 3a. The G-SSIM value of 0.90 for I_2 confirms this observation when I_5 is selected as reference. Furthermore, two small towers on the hilltop towards the right of the panorama are not easily distinguishable in Fig. 3b. However, when image I_1 is selected as the reference, these two small towers become clearer as the image contrast in increased, thus improving image detail and the quality of the overall panorama. When viewing such a panorama on large displays, such effects can get noticed easily. It is interesting to note that the reference chosen by [8] and [25] does not always results in a panorama with higher σ_{pano}. From our experiments, we set the thresholds of G-SSIM and $\Delta C_{\%age}$ to 0.95 and 15 %, respectively for all image sets. If the G-SSIM value of any image in the image sequence is less than 0.95 or the $\Delta C_{\%age}$ is greater than 15 %, that image is not set as the best color reference.

It can be argued to make use of image entropy as a ranking measure. Entropy is a statistical measure that is typically used to determine image texture [27] and is given by:

$$E = -\sum_{k=0}^{L-1} P_k \times \log_2 (P_k) \tag{7}$$

where P_k is the probability of the pixel value k in an image with L possible gray values. For sake of comparison, entropy of each image is also computed to analyze the suitability of the image characterized by highest value of E as I_{ref}. Thus, the Entropy value in Table 2 suggests I_3 as I_{ref} and the corresponding panoramic image is provided in Fig. 3c. Although there is no reduction in the image details, slightly washed out appearance of the hills at the right side (zoomed in for clarity) compared to the top-most panorama can be observed. Nevertheless, the reference selected by the proposed scheme results in a panorama with the maximum value of σ_{pano}.

Table 3 provides the comparative measures for office building panorama of Fig. 4. Panoramas a, b, and c provide the outputs for the cases when selected reference is I_4 (proposed by D), I_1, (proposed by [8]) and I_5, respectively. Here the proposed technique initially selects I_5, however the selection does not satisfy the conditions of the validation stage and as a result I_4 is automatically selected as the reference. The higher value of $\Delta C_{\%age}$ (19.4 %) or image I_3 when I_5 is reference reveals color clipping as the significant cause of decrease in its σ_{pano}. Furthermore, lower values of G-SSIM values for images I_1(0.89), I_2(0.91) and I_3(0.87) confirm significant loss of image details when I_5 is selected as reference. This can be verified visually by observing the highlighted rectangular region on the building face of Fig. 4c. The details of red bricks that are visible in panoramas of the Fig. 4a, b have been nearly effaced in the middle panorama. Hence, based on the two thresholds i.e., 0.95 for G-SSIM and 15 % for $\Delta C_{\%age}$, the selection of I_5 is automatically rejected. The next most suitable reference recommended by D is I_4, which meets the defined suitable reference criteria and is automatically selected by the proposed technique. Table 3 confirms that the reference selected by [8] and [25] does not result into panorama with maximum σ_{pano}. In Fig. 4b, the branches and leaves of the trees are not clear. However, due to improved contrast, the branches and leaves of the same trees are clearer in the panorama of Fig. 4a. As mentioned in Sect. 3, the G-SSIM threshold and $\Delta C_{\%age}$ thresholds

are decreased in steps in case no image meets the desired quality. For results discussed here, each of the threshold is decreased by 5 % when such a situation arises. This value of step size has been set empirically considering 5 % as a reasonable change representing a good trade-off between image quality and the time taken to converge upon a reference. This step size can be further reduced (as low as 1 %) to allow a more exhaustive search for the most suitable reference. In addition to this, the initial thresholds can also be modified and made stringent.

Table 4 provides the results for the Baseball stadium panorama of Fig. 5. For this panorama, the reference selected by the proposed scheme, [25] and [8] is same (Fig. 5a). Table 4 confirms that the value of σ_{pano} is maximum for the panorama generated using I_5 as the reference. The panorama of Fig. 5a has a higher contrast, making the pitch and the scoreboard overall brighter and richer in color when compared with that of Fig. 5b (with least value of D).

Table 5 provides the results for street panorama of Fig. 6. The proposed scheme selects I_5 as the reference while the scheme of [8] selects I_2 as the reference. It is important to note that I_2 is considered as the least suitable reference. Table 5 confirms that the panorama generated using I_5 as the reference results in a panorama with maximum σ_{pano} while, I_2 results in the panorama with least σ_{pano}. Also, the reference selected by [25] results in a lower value of σ_{pano} compared to the one by proposed scheme. Figure 6 confirms this observation. Figure 6b, which is the output of selecting the reference by [8], has a significantly lower contrast than that of Fig. 6a and has an overall dull appearance. In particular, the branches of the trees and the details of car park towards the right are clearly visible in Fig. 6a.

Table 6 provides the results for Island panorama of Fig. 7. The panorama of Fig. 7a, b are generated when I_4 (ranked most suitable by proposed scheme) and I_5 (selected by [8]) is selected as I_{ref}, respectively. Table 6 confirms that reference (I_5 and I_1) selected by [8] and [25] result into a panorama with lower σ_{Pano} as compared to the one generated using I_4. The highlighted region of Fig. 7b highlights a relatively washed out appearance of the island as compared to that of Fig. 7a, confirming to the results of Table 6.

Table 7 provides the results for Concert panoramas of Fig. 8. Table 7 confirms that the reference selected by proposed scheme and [8] provides a panorama with highest σ_{pano} while the one generated by [25] provides relatively lower σ_{pano}. The table further highlights that the least suitable color reference as suggested by the metric D results in a panorama with the lowest σ_{pano}, thus confirming the efficacy of the proposed measure.

The panorama of Fig. 8b, the least suitable reference, is dull and has low contrast. The panorama of Fig. 8a is brighter with higher contrast, as shown by the panorama standard deviations. In particular, the improvement in the contrast of hills (highlighted) in Fig. 8a compared to Fig. 8b can also be observed.

A subjective qualitative evaluation survey inspired from the pair comparison method (PC) of the ITU-T recommendation for quality assessment [28] was performed. PC method compares two alternative schemes at a time thus two surveys were carried out for comparison with [25] and [8]. Twenty participants were shown the panorama generated using the proposed reference selection scheme followed by the one generated using [25]. They were then asked to rate the better of the two results based upon their visual plausibility. The participants were also given the option of 'difference not discernible'. Each candidate had the option to view any panorama in an image set at will and was given the option to zoom into the native resolution as well. The same test was repeated for the comparison of proposed scheme with that of [8]. Figure 9a, b provide the results of this subjective evaluation for the panoramas shown in this work for [25] and [8], respectively.

From the bar chart of Fig. 9a we can observe that users voted convincingly for the proposed scheme as compared to [25] for university, fountain, office, street and Island panorama. The bar chart of Fig. 9b highlights that for university, fountain, street and Island the proposed scheme resulted in panorama that was voted as visually more plausible as compared to the one generated by [8]. For baseball stadium and Concert panorama, the computed reference was same for both the schemes and hence the majority voted for difference not discernable.

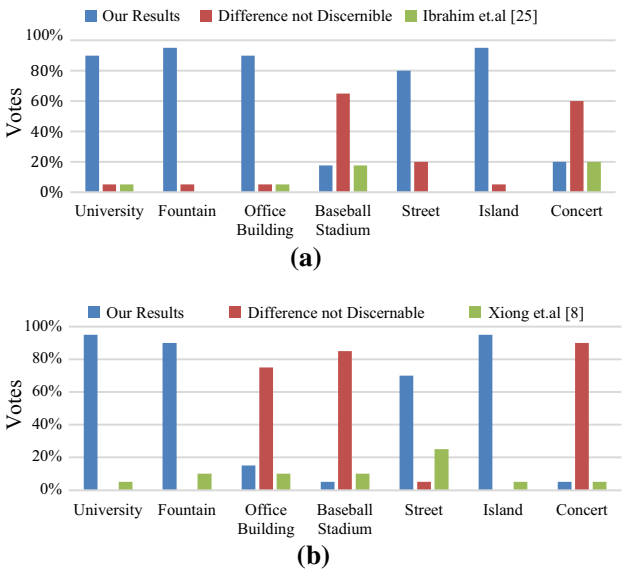

Fig. 9 PC based subjective comparison of panoramic images generated using I_{ref} selected by proposed scheme with that of **a** [25] and **b** [8]

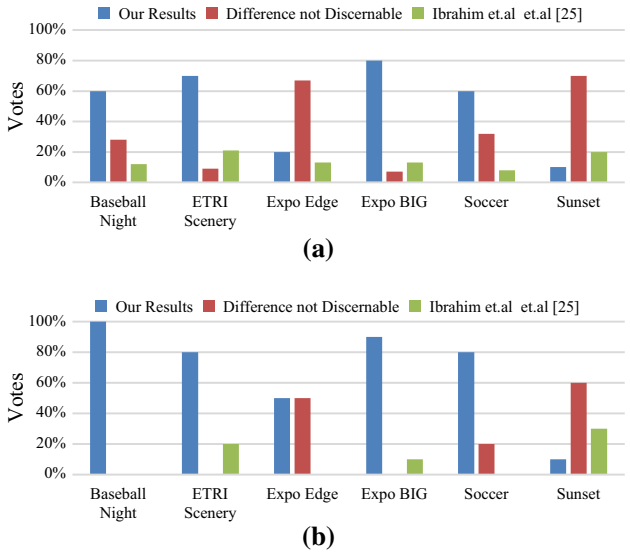

Fig. 10 PC based subjective comparison of panoramic videos generated using I_{ref} selected by proposed scheme with that of **a** [25] and **b** [8]

4.2 Results for panoramic videos

For panoramic videos, the parameters for geometric and photometric correction and the selection of I_{ref} were performed using the initial frame of each camera. For subsequent frames, these pre-computed parameters were employed to stitch the frames of panoramic video. An ITU-T inspired PC-based survey similar to the one above was thus performed for six panoramic videos. Each of these panoramic videos was stitched from seven synchronized video files acquired using a custom camera rig employing seven SONY FS100 cameras. Twenty participants were shown the panoramic videos generated using the proposed scheme followed by the video generated by employing the color reference suggested by the two schemes of [25] and [8]. KMPlayer was used by the candidates since it allowed simultaneous playing and zooming in of the panoramic videos. The test was performed using a 24″ DELL ST2420L monitor. Figure 10a, b provide the survey results for comparison with [25] and [8], respectively. The bar chart in Fig. 10a shows that for the baseball, ETRI Scenery and Expo BIG panoramic videos, the proposed scheme produced convincingly better results compared to those of [25]. The bar chart in Fig. 10b shows that for four out of six cases the majority of participants rated the results of proposed scheme as visually more pleasing compared to those of [8]. For one case (sunset) the majority could not appreciate the difference while a few users voted for the video produced by [8]. For Expo Edge panoramic video, either the candidates voted for the proposed scheme or they could not appreciate the difference.

4.3 Automatic reference selection for panoramic images using brightness transfer function [17] and gain compensation [1]

To demonstrate the applicability of the proposed scheme for color correction techniques other than Diagonal plus Affine model, the scheme was also tested for brightness transfer function [17], a non-parametric technique and gain compensation [1] a parametric technique. Our selection of these color correction schemes is inspired from Xu et al. [9] which rank these schemes as among the best. We have used the implementation of Xu et al. [9] for these techniques. For comparison, I_1 is assumed to be the arbitrarily selected reference and is compared against the automatically selected reference selected by the proposed scheme. Tables 8 and 9 provide the results for Office building (Fig. 11) and Concert panorama (Fig. 12), when the non-parametric color correction scheme of [17] is used. While I_5 has the largest value of D its selection is invalidated due to low G-SSIM value of I_1 and I_3. I_4 is thus automatically selected since it passes the validation criterion.

Tables 10 and 11 provide the results for office building (Fig. 13) and Concert panorama (Fig. 14), when the parametric color correction scheme of [1] is used. Both office building and Concert panoramas created using the proposed scheme exhibit better overall contrast in the output panorama compared to the least suitable reference.

Table 8 Values of D, G-SSIM, $\Delta C_{\%age}$ and σ_{pano} for each possible selection of I_{ref} for office building panorama of Fig. 11

I_{ref}	D	G-SSIM					$\Delta C_{\%age}$					σ_{pano}
		I_1	I_2	I_3	I_4	I_5	I_1	I_2	I_3	I_4	I_5	
I_1	0	1	0.99	0.96	0.94	0.81	0	0	0	0	0	12
I_2	9.03	0.99	1	0.97	0.96	0.85	0	0	0	0	0	10.58
I_3	5.32	0.99	0.97	1	0.93	0.76	0	0	0	0	0	12.33
I_4	107.15	0.93	0.97	0.94	1	0.96	0	0	0	0	0	11.24
I_5	140.76	0.87	0.91	0.84	0.98	1	0	0	0	0	0	10.57

Table 9 Values of D, G-SSIM, $\Delta C_{\%age}$ and σ_{pano} for each possible selection of I_{ref} for Concert panorama of Fig. 12

I_{ref}	D	G-SSIM					$\Delta C_{\%age}$					σ_{pano}
		I_1	I_2	I_3	I_4	I_5	I_1	I_2	I_3	I_4	I_5	
I_1	0	1	0.99	0.99	0.98	0.99	0	3.5	0.01	4.3	0.01	9.11
I_2	−35.59	0.99	1	0.99	0.99	0.98	−0.01	0	0	3.1	−0.02	8.74
I_3	−6.03	0.99	0.99	1	0.99	0.98	−0.01	0.34	0	3.9	−0.02	9.52
I_4	−53.89	0.96	0.99	0.97	1	0.97	−0.01	0	0	0	−0.02	8.1
I_5	14.8	0.99	0.99	0.99	0.97	1	0.01	0.46	0	4.22	0	9.62

Fig. 11 Generated Office building panoramas when: (*upper*) least suitable reference I_1 and (*lower*) most suitable reference I_4 is selected by proposed scheme

Fig. 12 Generated Concert panoramas when: (*upper*) least suitable reference I_4 and (l*ower*) most suitable reference I_5 is selected by proposed scheme

5 Conclusion

This paper presents a technique to automatically select and validate a color reference image that results in a panorama with higher standard deviation, hence appearing to have higher contrast and richer colors. D rates the image with highest relative standard deviation of the RGB channels in the overlapping region as the most favorable reference. Color correction scheme is then applied to all the images constituting the panorama. To ensure the visual plausibility of images; metrics of G-SSIM and $\Delta C_{\%age}$ are employed to measure the preservation of edges and the amount of clipping introduced in the RGB channels of the color corrected images due to application of the color correction approach. If all the images meet the G-SSIM and $\Delta C_{\%age}$ thresholds, the reference selection is validated; otherwise the next most suitable reference is selected and verified. In case no image meets the set thresholds, the thresholds are relaxed and the validation steps are repeated until a reference is selected, thereby completely automating the process. Experimentation was performed to prove the efficacy of proposed scheme for two parametric and one non-parametric color correction approach. The testing consisted of subjective evaluation based on ITU standards and of objective evaluation based on the measure of standard deviation. Detailed discussion on results demonstrated that the proposed scheme

Table 10 Values of D, G-SSIM, $\Delta C_{\%age}$ and σ_{pano} for each possible selection of I_{ref} for office building panorama of Fig. 13

I_{ref}	D	G-SSIM					$\Delta C_{\%age}$					σ_{pano}
		I_1	I_2	I_3	I_4	I_5	I_1	I_2	I_3	I_4	I_5	
I_1	0	1	0.99	0.99	0.99	0.93	0	−0.05	8.5	−0.11	−1.5	10.05
I_2	9.03	0.99	1	0.98	0.99	0.95	0.42	**0**	10.2	0.2	−1.5	10.64
I_3	5.32	0.99	0.98	1	0.96	0.88	−0.01	−0.05	0	−0.11	−1.5	10.11
I_4	107.15	0.99	0.99	0.96	1	0.97	2.2	0.41	14.1	0	−1.5	10.67
I_5	140.76	0.94	0.96	0.89	0.97	1	5.1	10.5	21.8	9.5	0	10.34

Table 11 Values of D, G-SSIM, $\Delta C_{\%age}$ and σ_{pano} for each possible selection of I_{ref} for Concert panorama of Fig. 14

I_{ref}	D	G-SSIM					$\Delta C_{\%age}$					σ_{pano}
		I_1	I_2	I_3	I_4	I_5	I_1	I_2	I_3	I_4	I_5	
I_1	0	1	0.99	0.97	0.98	0.96	0	3.1	0.11	4.0	0.21	9.23
I_2	−35.59	0.99	1	0.97	0.98	0.98	−0.03	0	0	2.1	−0.12	8.95
I_3	−6.03	0.98	0.99	1	0.98	0.98	−0.03	0.34	0	3.8	−0.01	9.67
I_4	−53.89	0.95	0.99	0.96	1	0.96	−0.02	0	1	0	−0.12	8.2
I_5	14.8	0.99	0.98	0.99	0.98	1	0.01	0.3	0	3	0	10.12

Fig. 13 Generated Office building panoramas when: (*upper*) least suitable reference I_1 and (*lower*) most suitable reference I_4 is selected by proposed scheme

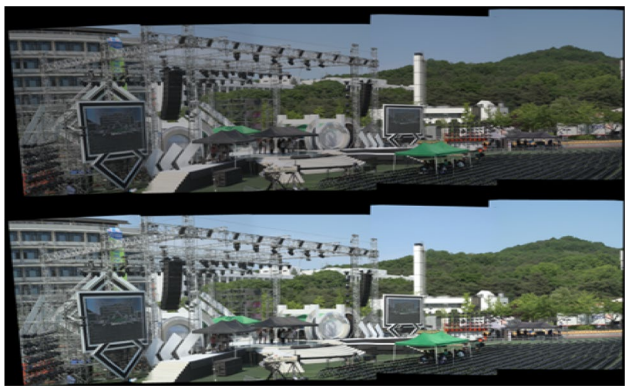

Fig. 14 Generated Concert panoramas when: (*upper*) least suitable reference I_4 and (*lower*) most suitable reference I_5 is selected by proposed scheme

yielded visually pleasing results for a number of panoramic images. The extendibility of scheme for panoramic videos is also demonstrated with the help of a subjective evaluation survey.

Acknowledgments We would like to thank IT R&D program of MKE/ETRI (14ZR1110, HCI-based UHD Panorama Technology Development) for their generous funding. NUST authors are also thankful to National ICT R&D Fund Pakistan for their support.

References

1. Brown, M., Lowe, D.G.: Automatic panoramic image stitching using invariant features. Int. J. Comput. Vision **74**(1), 59–73 (2007)
2. Fehn, C., Weissig, C., Feldmann, I., Müller, M., Eisert, P., Kauff, P., Blob, H.: Creation of high-resolution video panoramas for sport events. Int. J. Semant. Comput. (IJSC) **1**(2), 171–184 (2007)
3. Ikeda, S., Sato, T., Yokoya, N.: High-resolution panoramic movie generation from video streams acquired by an omnidirectional multi-camera system. In: Proceedings of IEEE international conference on multisensor fusion and integration for intelligent systems (MFI), pp. 155–160 (2003)
4. Gledhill, D., Tian, G.Y., Taylor, D., Clarke, D.: Panoramic imaging—a review. Comput Graph **27**(3), 435–445 (2003)
5. Majumder, A., Seales, W.B., Gopi, M., Fuchs, H.: Immersive teleconferencing: a new algorithm to generate seamless panoramic video imagery. In: Proceedings of seventh ACM international conference on multimedia, pp. 169–178 (1999)
6. Kimber, D., Foote, D.J., Lertsithichai, S.: Flyabout: spatially indexed panoramic video. In: Proceedings of ninth ACM international conference on multimedia, pp. 339–347 (2001)
7. Ladybug. http://ww2.ptgrey.com/products/ladybug5. Accessed Sep 2013
8. Xiong, Y., Pulli, K.: Fast Panorama stitching for high-quality panoramic images on mobile phones. IEEE Trans. Consum. Electron. **56**(2), 298–306 (2010)
9. Xu, W., Mulligan, J.: Performance evaluation of color correction approaches for automatic multi-view image and video stitching. In: Proceedings of IEEE computer vision and pattern recognition (CVPR), pp. 263–270 (2010)
10. Leigh, J., Johnson, A., Renambot, L., et al.: Scalable resolution display walls. Proc. IEEE **101**(1), 115–129 (2013)
11. Pirk, S., Cohen, M.F., Deussen, O., Uyttendaele, M., Kopf, J.: Video enhanced gigapixel panoramas. Proceedings of SIGGRAPH Asia 2012 Technical Briefs
12. Sargent, R., Bartley, C., Dille, P., Keller, J., Nourbakhsh, I., Grand, L.: Timelapse gigapan: capturing, sharing, and exploring timelapse gigapixel imagery. In: Proceedings of fine international conference on gigapixel imaging for science (2010)
13. Schreer, O., Feldmann, I., Weissig, C., Kauff, P., Schäfer, R.: Ultrahigh-resolution panoramic imaging for format-agnostic video production. In: Proceedings of the IEEE, vol. 101, no. 1, pp. 99–114 (2013)
14. Karen, A., Frenkel, : Panning for science. Science **330**, 748–749 (2010)
15. Chen, G.H., Yang, C.L., Xie, S.L.: Gradient-based structural similarity for image quality assessment. In: Proceedings of IEEE international conference on image processing, pp. 2929–2932 (2006)

16. Jia, J., Tang, C.K.: Image registration with global and local luminance alignment. In: Proceedings of 9th IEEE international conference on computer vision (ICCV), 1, pp. 156–163 (2003)
17. Kim, S.J., Pollefeys, M.: Robust radiometric calibration and vignetting correction. IEEE Trans. Pattern Anal. Mach. Intell. **30**(4), 562–576 (2008)
18. Tai, Y.W., Jia, J., Tang, C.K.: Local color transfer via probabilistic segmentation by expectation-maximization. Proc. IEEE Comput. Vision Pattern Recogn. (CVPR) **1**, 747–754 (2005)
19. Xiang, Y., Zou, B., Li, H.: Selective color transfer with multi-source images. Pattern Recogn. Lett. **30**(7), 682–689 (2009)
20. Xiong, Y., Pulli, K.: Fast and high-quality image blending on mobile phones. In: Proceedings of 7th IEEE consumer communications and networking conference (CCNC), pp. 1–5 (2010)
21. Tian, G.Y. , Gledhill, D., Taylor, D., Clarke, D.: Color correction for panoramic imaging. In: Proceedings of 6th international conference on information visualization, pp. 483–488 (2002)
22. Xiong, Y., Pulli, K.: Color matching for high-quality panoramic images on mobile phones. IEEE Trans. Consum. Electron. **56**(4), 2592–2600 (2010)
23. Xiong, Y., Pulli, K.: Fast image stitching and editing for panorama painting on mobile phones. In: IEEE computer vision and pattern recognition workshops (CVPRW), pp. 47–52 (2010)
24. Doutre, C., Nasiopoulos, P.: Fast vignetting correction and color matching for panoramic image stitching. In: Proceedings of 16th IEEE international conference on image processing (ICIP), pp. 709–712 (2009)
25. Ibrahim, M.T., Hafiz, R., Khan, M.M., Cho, Y., Cha, J.: Automatic reference selection for parametric color correction schemes for panoramic video stitching. In: International symposium on visual computing, Part 1, LNCS 7431, pp. 492–501 (2012)
26. Wang, Z., Bovik, A.C., Sheikh, H.R., Simoncelli, E.P.: Image quality assessment: from error measurement to structural similarity. IEEE transactions on image processing, vol. 13, no. 1 (2004)
27. Annadurai, S., Shanmugalakshmi, R.: Fundamentals of digital image processing, pp. 155 (2007)
28. ITU-T Recommendation: Subjective video quality assessment methods for multimedia applications (2008)
29. Sheikh, H.R., Bovik, A.C.: Image information and visual quality. IEEE Trans. Image Process. **15**(2), 430–444 (2006)
30. Wang, Z., Bovik, A.C.: A universal image quality index. Signal Process. Lett. IEEE **9**(3), 81–84 (2002)